Rheologica Acta (2022) 61:799–809
https://doi.org/10.1007/s00397-022-01374-9

ORIGINAL CONTRIBUTION

Comparison of shear viscosity and normal stress measurements by rotational and on-line slit rheometers with tube model predictions

Paulo F. Teixeira[1] · Loic Hilliou[1] · Jose A. Covas[1] · Esmaeil Narimissa[2,3] · Leslie Poh[2,3] · Manfred H. Wagner[4]

Received: 28 June 2022 / Revised: 30 August 2022 / Accepted: 17 October 2022 / Published online: 12 November 2022

Abstract

In-extruder measurements of shear viscosity and normal stresses are important as these measurement techniques allow determining the rheological state of the polymer melt at processing conditions up to high shear rates. However, validation of viscosity and normal stress data obtained by in-line slit rheometers at high shear rates is difficult due to a lack of overlap of the in-line data and the off-line measurements by rotational rheometers limited to lower shear rates. Here, shear viscosity and normal stress data measured in-line at large shear rates during extrusion and off-line at low shear rates are compared to predictions of the Doi-Edwards model and the Hierarchical Multi-Mode Molecular Stress Function (HMMSF) model using linear-viscoelastic off-line small amplitude oscillating shear data of two polystyrenes and a low-density polyethylene as input parameters. For polystyrene, the results of this investigation do not only validate the experimental data obtained by rotational as well as slit-die rheometry, but also demonstrate the agreement between experiments and models up to very high shear rates, which were not experimentally accessible earlier. The low-density polyethylene shows a more complex behaviour, which follows the HMMSF model at low shear rates, but approaches the Doi-Edwards model at high shear rates.

Keywords In-process rheometer · Slit die · Shear viscosity · Normal stress difference · Doi-Edwards model · HMMSF model

Introduction

Polymer melt extrusion is at the core of plastics processing. Extruders are used for compounding as well as for modifying and/or blending polymers, often by reactive extrusion. Extruders are also used to convert compounds into sheets, films, pipes and tubing, profiles, etc. Melt extrusion requires specific melt viscoelastic properties to ensure good quality extrudates, with smooth surface and proper dimensions, at high production rates. The rheological characterization and modelling of polymer melts at large shear rates in the nonlinear viscoelastic regime is thus of high practical relevance, namely for assessing their processability and predicting extrusion instabilities (see, e.g., Dealy 2005; Cyriac et al. 2013).

Rotational rheometry is a well-established technique for measuring the steady-state rheological functions of interest, which are essentially shear viscosity and normal stress differences. However, at high shear rates, secondary flow instabilities develop due to large first and second normal stress differences which drive surface distortion (Kulicke et al. 1979) and edge fracture (Tanner and Keentok 1989), respectively. The cone-partitioned plate (CPP) geometry has been introduced to mitigate the effects of these instabilities (Meissner et al. 1989; Schweizer 2002; Snijkers and Vlassopoulos 2011), but the large torques generated at very high shear rates reach the limits of torque transducers of commercial rotational rheometers. Thus, in practice, measurements

✉ Jose A. Covas
jcovas@dep.uminho.pt

✉ Manfred H. Wagner
manfred.wagner@tu-berlin.de

1 Institute for Polymers and Composites, University of Minho, 4800-058 Guimarães, Portugal

2 Department of Chemical Engineering, Technion–Israel Institute of Technology (IIT), Technion City, 32 000 Haifa, Israel

3 Department of Chemical Engineering, Guangdong Technion–Israel Institute of Technology (GTIIT), 515063 Shantou, China

4 Polymer Engineering/Polymer Physics, Berlin Institute of Technology (TU Berlin), Ernst-Reuter-Platz 1, 10587 Berlin, Germany

at shear rates exceeding 100 s^{-1} are challenging for highly elastic melts (Schweizer 2002, 2003; Snijkers and Vlassopoulos 2011; Costanzo et al. 2018; You and Yu 2021) such as extrusion grade polymers.

The hole-pressure method (Broadbent et al. 1968) is an alternative route to assess both shear viscosity and normal stresses and can be used in in-process rheometers. The concept is illustrated in Fig. 1 for the specific case of slit rheometry. For each flow rate in the slit with height H, the shear viscosity η is inferred from the difference between the pressures P3 and P1 measured by two flush-mounted transducers on the slit, whereas normal stresses are acquired through the difference between P1 and the pressure P2, which is measured by a transducer mounted in the recess opposite to P1. A rectangular recess with depth d and width b gives access to the first normal stress difference N_1, whereas the second normal stress difference N_2 is measured with a circular recess, using the relationships between P3, P1, and P2 given by the Higashitani and Pritchard (1972) and Baird (1975) equations. With the correct choice of the slit and recess geometries, both shear viscosity and first normal stress difference could be accurately measured for commercial polyethylene and polystyrene melts at shear rates in the range of 10 to 300 s^{-1} (Teixeira et al. 2013, 2015a). However, N_2 measurements showed up to be practically unfeasible for these melts (Teixeira et al. 2013), whereas less elastic materials such as liquid crystalline polymers in the nematic phase (Teixeira et al. 2015a) do not generate sufficient hole-pressure at P2 to give a measureable N_1.

With the conventional slit die design displayed in Fig. 1, only a single point of the flow curve (η or N_1 vs. shear rate) is obtained at a specific operating condition (Baird 2008). The screw speed (single screw extruder) or the feed rate (twin screw extruder) must be changed to generate different shear rates in the measuring slit. Simultaneously, the residence time and stresses experienced by the material in the extruder will be also altered. In the case of multiphase materials such as polymer blends (Teixeira et al. 2015b), polymer nanocomposites, and thermo-mechanically sensitive materials such as bio-based and biodegradable polymers, this will cause changes in the material characteristics, i.e., a different material may be pumped to the measuring slit at each different shear rate. To bypass this problem, a double-slit design has been developed, whereby the melt exiting the extruder enters a measuring channel and a production channel (see Fig. 2). The flow in each channel can be regulated by a vertical valve at its entrance. Hence, by manipulating simultaneously the two valves in opposite directions, different flow rates can be generated in the two channels while maintaining the same operating conditions in the extruder (Teixeira et al. 2018).

It is worth noting that the set-up illustrated in Fig. 2 is unique in establishing relationships between extrusion conditions and flow curves. In short, the advantage of the double-slit die over the single-slit rheometer is that it can produce a flow curve without changing the extrusion conditions (screw speed or feed rate) to generate different shear rates in the slit. Indeed, when using off-line rotational rheometry to characterize the extrudates, the extra thermal cycles associated to disk preparation of the samples and loading in the rheometer might change the morphology of the material due to possible coalescence of the dispersed phase, degradation, or chemical reactions between the ingredients (Teixeira et al. 2020, 2021).

The in-line rheometers presented in Figs. 1 and 2 were validated by a direct comparison with the viscosity flow curves measured by off-line capillary rheometry performed on rheologically simple systems such as industrial polystyrene and polyethylene melts (Teixeira et al. 2013, 2018). However, these materials were too elastic to allow for normal stress measurement with rotational

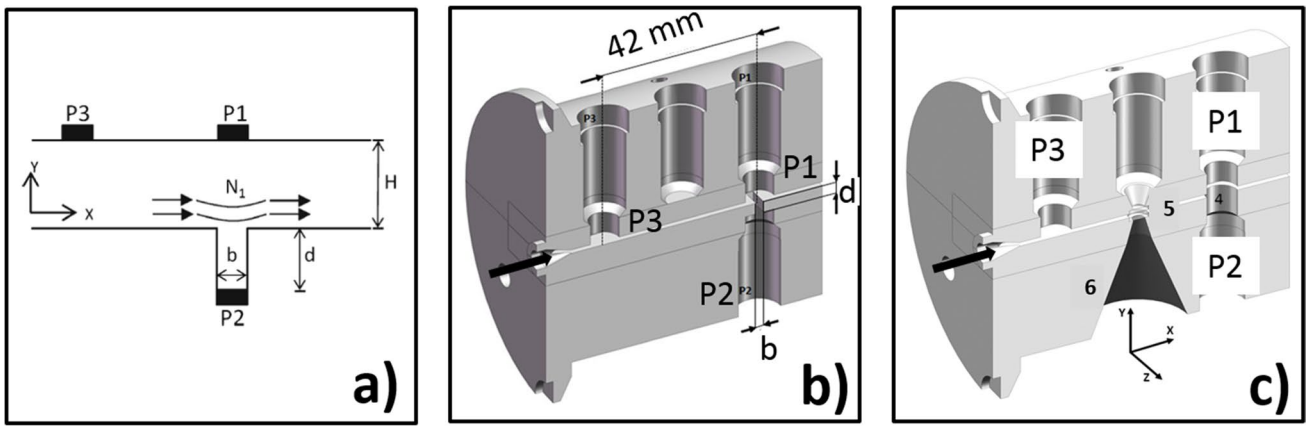

Fig. 1 Schematic representation of the hole-pressure method (**a**) and design of slit dies for the simultaneous measurement of η, N_1 (**b**, with rectangular recess) or N_2 (**c**, with circular recess (4)). The thick black arrow in (**b**) and (**c**) indicates the flow of material from the extruder outlet to the slit die inlet, whereas optical windows (5) and aperture for optical measurements (6) are indicated in (**c**)

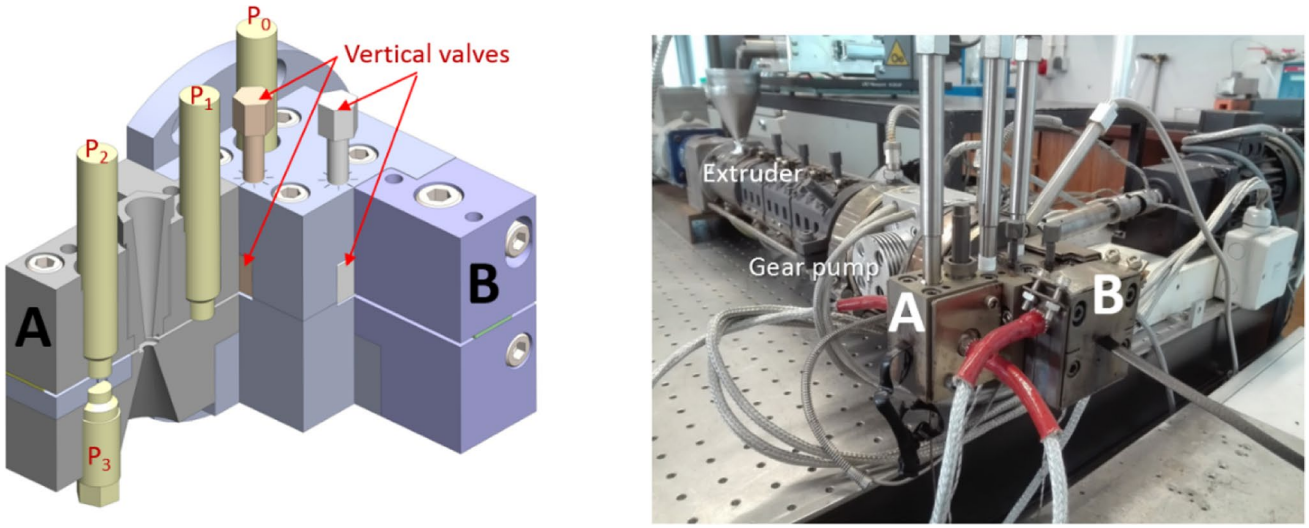

Fig. 2 Schematic representation of the double-slit rheological die (left) and photo of the actual die coupled to a prototype mini-scale twin-screw co-rotating extruder (right) taken during the compounding of a carbon-based polymer nanocomposite (Infurna et al. 2020). P_0 indicates the location of the pressure transducer used to monitor the pressure at the output of the extruder, which is kept constant by balancing the flows in the measuring (**A**) and the production (**B**) channels using vertical valves located at both channels entrances. The measuring channel (A) reproduces the design displayed in Fig. 1 for the hole-pressure method with optical access for light scattering, microscopy, or turbidity measurement

rheometry at shear rates overlapping those achieved with the in-line slit or double-slit rheometers. So far, the confidence in the validity of the measured N_1 data at high shear rates could only be based on comparison to Laun's empirical relationship with the frequency dependence of the storage modulus $G'(\omega)$ (Laun 1986). In this paper, a comparison of the experimental data obtained by off-line (rotational) rheometers in the low shear-rate regime and by the in-line rheometers in the high shear-rate regime with predictions of tube models for entangled polymer melts, the Doi-Edwards model (Doi and Edwards 1978), and the Hierarchical Multi-mode Molecular Stress Function (HMMSF) model (Narimissa et al. 2015, 2016; Narimissa and Wagner 2016a, b, c, 2018, 2019) is presented. The HMMSF is based on a few well-defined rheological assumptions and has been shown to model accurately the rheology of polydisperse linear and branched polymer melts in extensional and shear flows with only one or two nonlinear material parameters. However, the comparison of experimental data and HMMSF model in shear flow was so far restricted to linear (HDPE) and long-chain branched (LDPE) polyethylenes at shear rates up to 10 s^{-1} (Narimissa and Wagner 2016a, c).

The objective of this paper is thus twofold: (i) To compare the rotational, slit, and double-slit rheometer data with the predictions of the Doi-Edwards and the HMMSF model, and (ii) to test the model predictions for shear viscosity and normal stresses with experimental data of commercial polymers processed under industrial (lab-scale) conditions at shear rates up to 3000 s^{-1} and 300 s^{-1}, respectively.

Materials and methods

Materials

For experiments with the set-up displayed in Fig. 1, a polystyrene (PS) Edistir N2560 from Polimeri Europa and a low-density polyethylene (LDPE) Lupolen 1840H from BASF were used. A polystyrene (PS) RXP 3002 Natural from Resinex was used to validate the double-slit in-line rheometer presented in Fig. 2. This commercial plastic has a melt flow index of 11 g/10 min (200 °C/5.0 kg).

Rheometry

Detail about the calibration of the pressure transducers and their mounting on the measuring slit was given elsewhere (Teixeira et al. 2013). The slit rheometer displayed in Fig. 1 was coupled to a capillary rheometer (Rosand RH10) in view to feed the polymer melts into the measuring channel under steady flow conditions. The method for producing flow curves with the slit rheometer coupled to the capillary rheometer has been detailed elsewhere (Teixeira et al. 2013). The Rosand RH10 capillary rheometer was also used to produce the shear viscosity data for PS Edistir N2560 at 190 °C and at shear rates overlapping and exceeding those achieved with the double-slit rheometer.

In-extruder experiments with the double-slit rheometer were conducted at constant extrusion conditions (screw speed or feed rate), each point in the flow curve being obtained with a given combination of the positions of the valves used to set the flow rates in the corresponding channels. The experimental set-up and methodology to produce flow curves were described in detail elsewhere (Teixeira et al. 2018).

Rotational rheometry was performed with a stress-controlled ARG2 rheometer (TA instruments) equipped with a 25-mm plate-plate geometry, and with two Advanced Rheometric Expansion System rheometers (ARES, TA Instruments) coupled to a cone-and-plate geometry (25-mm diameter and 0.1 rad cone angle) or a 25-mm plate-plate geometry. These were used in order to produce the linear viscoelastic data needed as input for the HMMSF model, and to compare η, N_1, and $N_1 - N_2$ values with model predictions at lower shear rates of the flow curves. Additional flow curves were obtained from two Advanced Rheometric Expansion System rheometers (ARES, TA Instruments) in two different laboratories (Polymeric Materials Group at the Karlsruhe Institute of Technology, Germany, indicated as "KIT" in the figures, and Applied Rheology and Processing Section at the Katholieke University of Leuven, Belgium, indicated as "KUL"). For experimental details, see Teixeira et al. (2013, 2018).

Modelling

The Hierarchical Multi-Mode Molecular Stress Function (HMMSF) model was developed by Narimissa and Wagner for the prediction of uniaxial (Narimissa et al. 2015), multiaxial (Narimissa et al. 2016), and shear (Narimissa and Wagner 2016a) rheological behaviours of polydisperse long-chain branched (LCB) polymer melts as well as polydisperse linear melts (Narimissa and Wagner 2016b, c). A summary of development of the HMMSF model was presented by Narimissa and Wagner (2018), a comparison between this model and other prominent tube-models for polydisperse linear and long-chain branched polymer melts was given by Narimissa and Wagner (2019), and a recent extension for elongational flow of LCB polymers by Wagner et al. (2022).

We shortly summarize the basic equations of the HMMSF model:

The extra stress tensor of the HMMSF is given by,

$$\sigma(t) = \sum_i \int_{-\infty}^{+\infty} \frac{\partial G_i\left(t-t'\right)}{\partial t'} f_i^2\left(t,t'\right) \mathbf{S}_{DE}^{IA}\left(t,t'\right) dt' \tag{1}$$

The extra stress is a sum over all stress contributions from discrete Maxwell modes making up the relaxation modulus,

$$G(t) = \sum_i G_i(t) = \sum_i g_i \exp\left(t/\tau_i\right) \tag{2}$$

with partial relaxation moduli g_i and relaxation times τ_i.

$\mathbf{S}_{DE}^{IA}$ is the Doi and Edwards orientation tensor with the independent alignment (IA) assumption (Doi and Edwards 1978), which is equal to 5 times the second-order orientation tensor $\mathbf{S}$.

The molecular stress functions $f_i = f_i\left(t,t'\right)$ are functions of observation time t and the time of creation of tube segments by reptation at time t', and are obtained by integration of the evolution equations,

$$\frac{\partial f_i}{\partial t} = f_i(\mathbf{K};\mathbf{S}) - \frac{1}{\alpha}\left(\frac{1}{\tau_i} + \beta CR\right)\left[\left(f_i - 1\right)\left(1 - \frac{2}{3}w_i^2\right) + \frac{2}{9}f_i^2\left(f_i^3 - 1\right)w_i^2\right] \tag{3}$$

$\mathbf{K}$ is the velocity gradient tensor and α a topological parameter which depends on the architecture of the chain,

$$\begin{aligned} &\alpha = 1 \ \text{ for LCB melts} \\ &\alpha = 1/3 \ \text{ for Linear melts} \end{aligned} \tag{4}$$

CR is a dissipative Constraint Release term which has nonzero values only in shear flow (CR = 0 in extensional flow) and can be expressed in terms of shear rate $\dot{\gamma}$ and the normal components of the orientation tensor $\mathbf{S}$ as $\mathrm{CR} = \frac{1}{2}\sqrt{\dot{\gamma}^2\left|S_{11} - S_{22}\right|}$. β is a numerical parameter which is determined experimentally.

The mass fractions w_i of chain segments in the evolution Eq. (3) take into account hierarchical relaxation and are determined by,

$$\begin{aligned} &w_i^2 = \frac{G(t=\tau_i)}{G_D} = \frac{1}{G_D}\sum_{j=1}^{n} g_j \exp\left(-\tau_i/\tau_j\right) \quad \text{for} \tau_i > \tau_D \\ &w_i^2 = 1 \qquad\qquad\qquad\qquad\qquad\qquad\quad \text{for } \tau_i \le \tau_D \end{aligned} \ ; \tag{5}$$

The mass fractions w_i of dynamically diluted segments with relaxation time τ_i longer than the dilution relaxation time τ_D are smaller than 1, while the mass fractions of permanently diluted segments with $\tau_i \le \tau_D$ are set equal to 1. G_D is called the "dilution modulus" and is a free parameter of the model.

The HMMSF model requires only a single fitting parameter for extensional flow (i.e., G_D) and an additional CR parameter (β) for shear flow.

The Doi-Edwards model with the independent alignment assumption (DEIA) is recovered from Eq. (1) by setting $f_i^2 \equiv 1$ (Doi and Edwards 1978). We will also test a combination of the HMMSF model and the DEIA model by use of Eq. (1), but assuming that polymer chain segments with relaxation times τ_i below a certain threshold value τ_c are so short that they are only oriented, but not stretched, i.e., that

$$f_i^2 \equiv 1 \ \ if\, \tau_i < \tau_c \tag{6}$$

We call this the "HMMSF-IA" model in the following.

Results and discussion

Linear-viscoelastic characterization

From small amplitude oscillatory shear (SAOS) experiments (Fig. 3), the relaxation spectra of PS Edistir N2560 at 190 °C, PS RXP 3002 at 210 °C, and LDPE 1840H at 150 °C were determined by the IRIS software (Winter and Mours 2006; Poh et al. 2022), and are summarized in Table 1.

Shear viscosity

The shear viscosity of the two polystyrene melts and the low-density polyethylene melt measured by rotational, capillary, and slit die rheometry up to shear rates of 1000–3000 s^{-1} are presented by symbols in Figs. 4 and 5. As far as the shear rate regimes of the different measurement methods overlap, general agreement of the experimental data was obtained. Predictions of the DEIA and the HMMSF models are indicated in the figures by lines. For the two polystyrene melts (Fig. 4), good agreement between experimental data and predictions of the DEIA model is found. This is consistent with a recent analysis of the steady-state shear viscosity of several monodisperse PS melts (Narimissa et al. 2020). Concerning the HMMSF model, we use a dilution modulus of $G_D = 7,000 Pa$ for both polystyrenes, which has been shown earlier (Narimissa and Wagner 2016c) to give excellent agreement with uniaxial and equibiaxial extensional flow data of a commercial PS melt (PS158K of BASF AG). We recall that the dissipative Constraint Release (CR) for shear flow of linear polymers such as polystyrene is large and use a CR parameter of $\beta = 1$ here. Predictions of the HMMSF model are therefore only slightly larger than those of the DEIA model, and are within experimental accuracy in good agreement with the experimental data.

Figure 5 presents the shear viscosity of LDPE 1840H measured by rotational, capillary, and slit die rheometry up to shear rates nearly 2000s^{-1}. Considering the wide range of shear rates investigated, good agreement of the different experimental methods is found. In the shear rate range between 10^{-2} and 1 s^{-1}, the DEIA model is slightly underpredicting the experimental data, while the high shear-rate predictions are in agreement with the measurements by capillary and slit die rheometry. On the other hand, the HMMSF model with a dilution modulus of $G_D = 10,000 Pa$

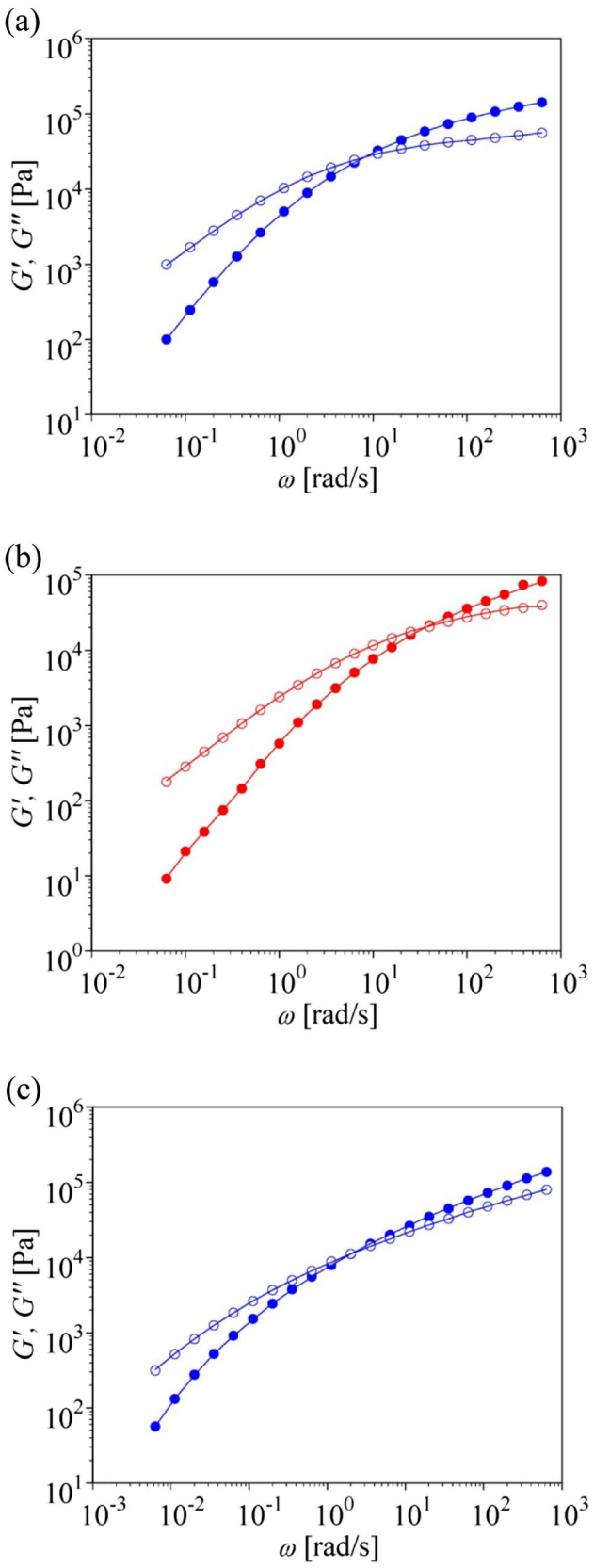

Fig. 3 Storage (G') and loss (G'') modulus of (**a**) PS Edistir N2560 at 190 °C, (**b**) PS RXP 3002 at 210 °C, and (**c**) LDPE 1840H at 150 °C. Lines are fit by parsimonious spectra of Table 1

Table 1 Relaxation spectra of PS Edistir N2560 at 190 °C, PS RXP 3002 at 210 °C, and LDPE 1840H at 150 °C

PS Edistir N2560		PS RXP 3002		LDPE 1840H	
g_i (Pa)	τ_i (s)	g_i (Pa)	τ_i (s)	g_i (Pa)	τ_i (s)
1.173e+005	5.359e−004	6.448e+004	1.553e−003	1.909e+005	4.786e−004
4.924e+004	4.139e−003	2.819e+004	8.471e−003	5.748e+004	3.208e−003
4.156e+004	2.007e−002	1.671e+004	3.996e−002	3.514e+004	1.405e−002
2.923e+004	8.951e−002	5.365e+003	1.745e−001	2.156e+004	6.394e−002
1.338e+004	3.899e−001	1.015e+003	7.594e−001	1.120e+004	3.101e−001
2.947e+003	1.710e+000	3.466e+001	7.510e+000	5.208e+003	1.338e+000
2.316e+002	9.043e+000			2.292e+003	5.664e+000
				6.772e+002	2.602e+001
				1.177e+002	1.053e+002

and a CR parameter of $\beta = 0.5$ results in good shear viscosity predictions within experimental accuracy in the full shear-rate range investigated (Fig. 5a). A dilution modulus of $G_D = 10,000Pa$ has already been shown earlier to result in an excellent description of the elongational viscosity for LDPE 1840H [Wagner 2022]. Predictions of the HMMSF-IA model, which becomes important in modelling the normal stress difference data (see below), are shown in Fig. 5b. Using a cut-off relaxation time of $\tau_c = 2s^{-1}$ for polymer chain stretch according to Eq. (6), agreement with the experimental data in the low shear-rate range between 10^{-2} and 1 s^{-1}, and convergence to the DEIA model predictions at high shear rates is obtained.

Normal stress differences

Figure 6 shows the normal stress differences of PS Edistir N2560 measured by rotational and slit die rheometers. While rotational rheometry is limited to shear rates up to 1 s^{-1}, the slit die rheometers cover the shear-rate range from 10 to 300 s^{-1}. As in the case of shear viscosity, good agreement between experimental data of the first normal stress difference and computed N_1 data from the DEIA model is found in the full range of shear rates investigated (Fig. 6a), and again this is consistent with the recent analysis of the steady-state first normal stress difference of several monodisperse PS melts (Narimissa et al. 2020). The HMMSF model with a dilution modulus of $G_D = 7,000Pa$ and a CR parameter of $\beta = 1$ are slightly larger than predictions of the DEIA model for N_1, but are clearly within experimental accuracy in good agreement with the experimental data.

Concerning the difference of the first and second normal stress differences (Fig. 6b), while predictions of both DEIA and HMMSF agree with the rotational measurements, the experimental data of $N_1 - N_2$ obtained by the slit-die circular slot technique at high shear rates are increasingly lower than predicted by the models. This points towards the difficulty in accurately measuring N_2 with the hole-pressure method, as established elsewhere (Teixeira et al. 2013).

The normal stress differences of PS PXP 3002 measured by rotational rheometers and the double-slit die rheometer are shown in Fig. 7. While agreement with predictions of the DEIA and HMMSF models is seen for the low shear rate rotational measurements of $N_1 - N_2$, the double-slit die measurements give only a very rough estimation of N_1.

The normal stress differences of LDPE 1840H measured by rotational and slit die rheometers are presented in Fig. 8. While rotational rheometry is limited to shear rates up to 10 s^{-1}, the slit die rheometers cover the shear rate range from 10 to 300 s^{-1}. The DEIA model clearly underpredicts the low shear rate range, but reasonable agreement between N_1 data and prediction in the range of high shear rates accessible by the slit-die rheometer is achieved (Fig. 8a). It may come as a surprise that the DEIA model gives not only a quantitative prediction of the N_1 data of the linear PS melts, but also of the N_1 data of the long-chain branched LDPE 1840D at high shear rates. However, this is in line with earlier findings of Ianniruberto and Marrucci (2013) that due to arm withdrawal, entangled melts of branched PS behave like linear PS in the steady state of fast elongational flows. The effect of arm withdrawal is most likely also the root cause of the agreement of the N_1 data of LDPE 1840H and the prediction of the DEIA model at high shear rates. We further note that as in the case of the polystyrene melt, the experimental data of $N_1 - N_2$ obtained by the slit-die circular slot technique are increasingly lower than predicted by the DEIA model (Fig. 8b).

In contrast to the DEIA model, the HMMSF model with a dilution modulus of $G_D = 10,000Pa$ and a dissipative CR parameter of $\beta = 0.05$ results in good agreement with experimental N_1 (Fig. 8a) and $N_1 - N_2$ data (Fig. 8b) in the low shear rate range up to a shear rate of about 1 s^{-1}, while a considerable deviation at high shear

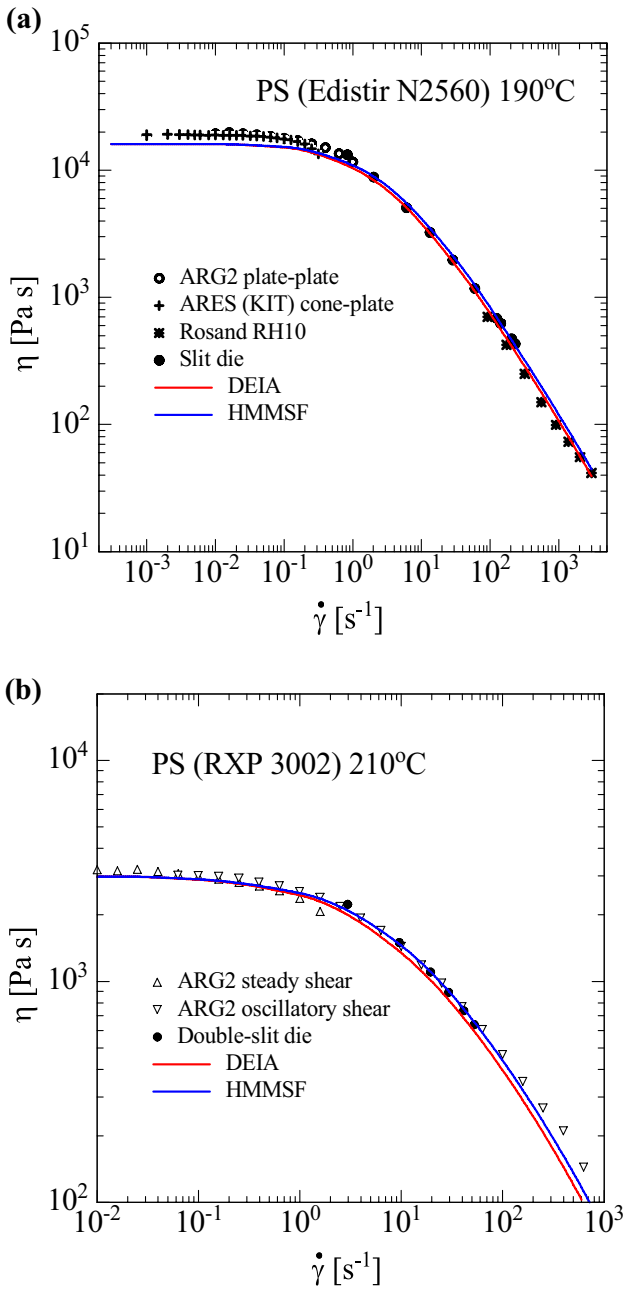

Fig. 4 Viscosity versus shear rate for (**a**) PS Edistir N2560 and (**b**) PS RXP 3002

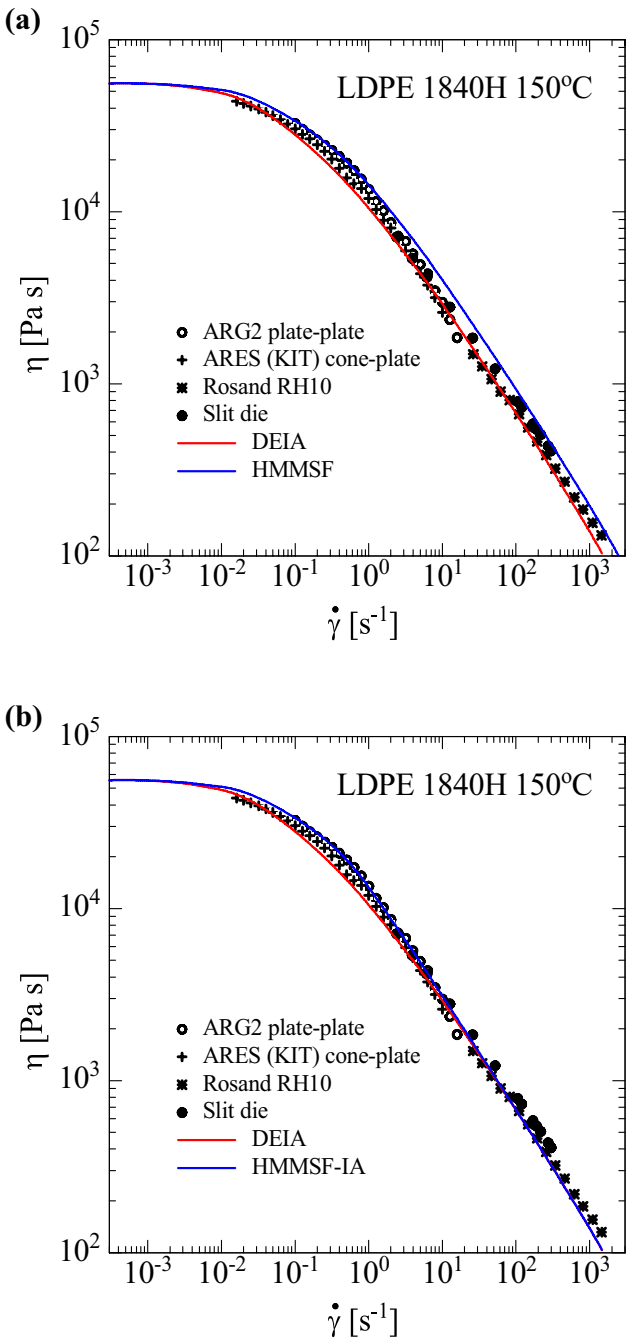

Fig. 5 Viscosity versus shear rate for LDPE 1840H. Lines indicate (**a**) predictions of the DEIA and HMMSF models; (**b**) predictions of the DEIA and HMMSF-IA models

rates is obvious. This deviation between model and data can be mitigated by assuming that polymer chain segments with relaxation times τ_i below a threshold value of $\tau_c = 2s$ are so short that they are only oriented, but not stretched, as in the HMMSF-IA model, which is a cross-over between the HMMSF and the DEIA model. Note that the value of $\tau_c = 2s$ corresponds to a shear rate of $\dot{\gamma}_c = 0.5s^{-1}$, which is approximately the shear rate when the slope of the normal stress curves starts to decrease. Indeed, this assumption leads to a transition between the low shear-rate HMMSF and the high shear-rate DEIA prediction. While the HMMSF-IA model results in an improved description of the experimental N_1 data in the full range of shear rates investigated (Fig. 8c), the deviations between model and the $N_1 - N_2$ data persist in the high shear-rate range (Fig. 8d).

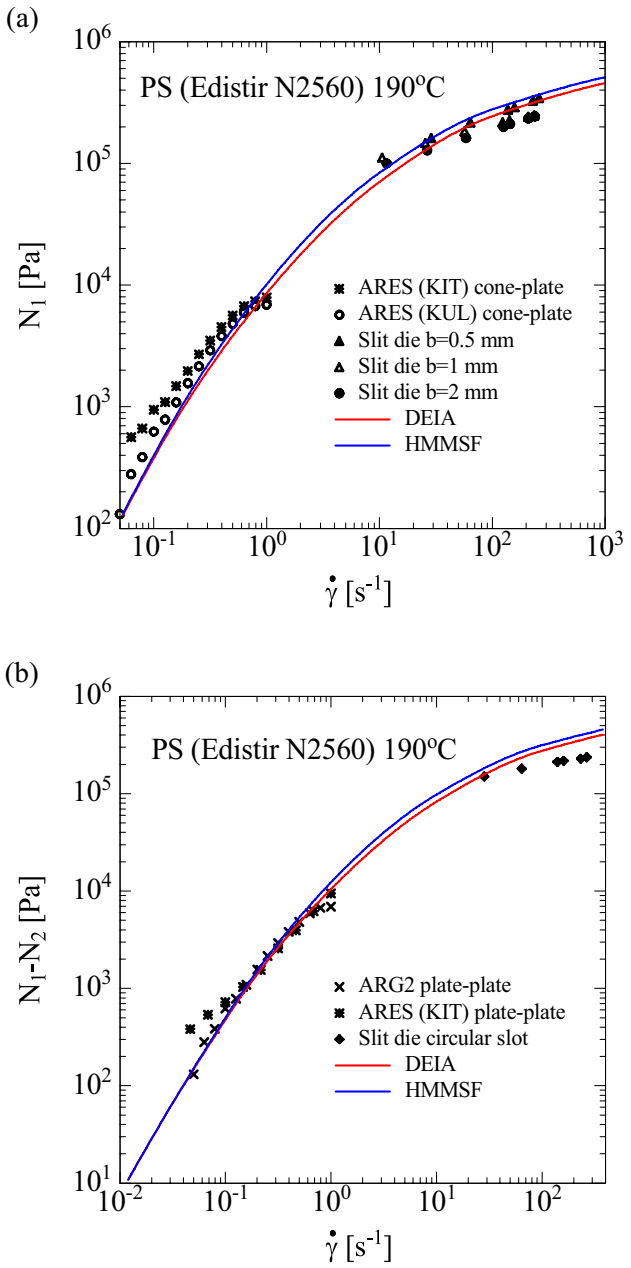

Fig. 6 Normal stress differences versus shear rate for PS Edistir N2560. (**a**) N_1; (**b**) $N_1 - N_2$

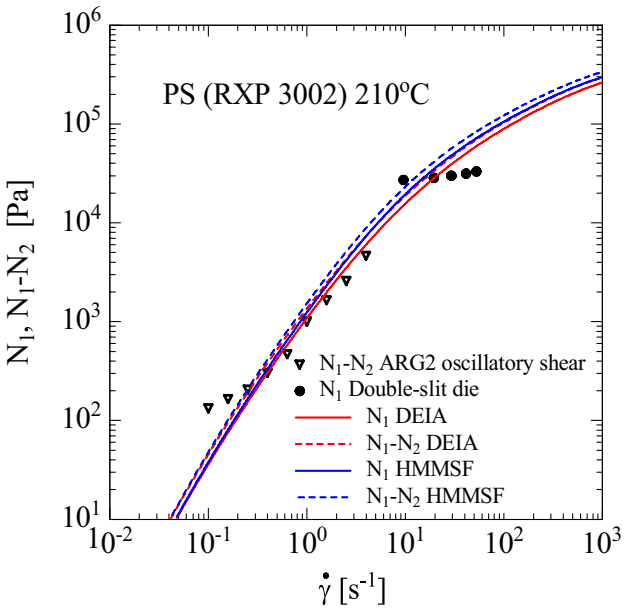

Fig. 7 Normal stress differences N_1 and $N_1 - N_2$ versus shear rate for PS RXP 3002

Conclusions

The comparison of the experimental data obtained by off-line (rotational) rheometers in the low shear-rate regime and by the in-line rheometers in the high shear-rate regime with predictions of tube-based models for entangled polymer melts leads to a number of interesting conclusions:

For polystyrene, the DEIA and the HMMSF models give accurate descriptions of shear viscosity and first normal stress difference N_1 for shear rates up to 3000 s^{-1} and 300 s^{-1}, respectively. This is an important result, which on the one side validates the experimental data obtained by rotational as well as slit-die rheometry, but also demonstrates the agreement between experiments and models up to very high shear rates, which were not experimentally accessible earlier. It is equally important that modeling works for the industrial polymers investigated here. Due to the high dissipative Constraint Release in shear flow of linear polymers, predictions of the HMMSF model are only marginally larger than predictions of the DEIA model and are in good agreement with the experimental data within experimental accuracy. However, we note that the HMMSF model with the same parameter of the dilution modulus for polystyrene as used here has been shown earlier (Narimissa and Wagner 2016c) to give excellent agreement with uniaxial and equibiaxial extensional flow data, while the DEIA model fails utterly in extensional flows. Therefore, the HMMSF model can be used in 3D simulations of complex flows in polymer processing combining both extensional and shear flows such as in the case of abrupt contraction flow (Olley et al. 2022).

In the case of $N_1 - N_2$, the agreement between experimental data for polystyrene and predictions of the DEIA and HMMSF models is restricted to data obtained by rotational rheometry at shear rates up to 1 s^{-1}, while the

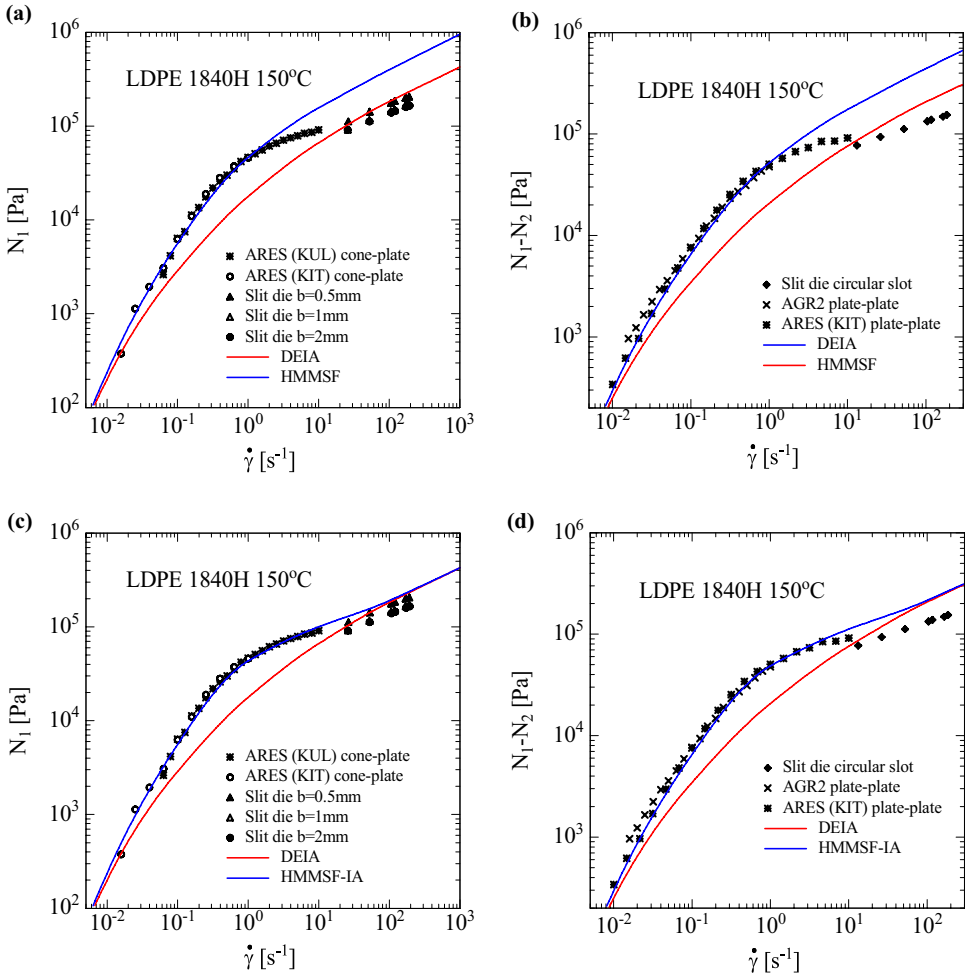

Fig. 8 Normal stress differences N_1 and $N_1 - N_2$ versus shear rate for LDPE 1840H. Lines indicate (**a**) and (**b**) predictions of the DEIA and HMMSF models; (**c**) and (**d**) predictions of the DEIA and HMMSF-IA models

slit-die circular slot rheometry shows larger deviations from the predictions of the models.

For long-chain branched polymer melts such as the LDPE investigated here, which are known to feature strong strain hardening in extensional flows, the DEIA model shows a small underprediction of the shear viscosity at low shear rates as well as a strong underprediction of the first normal stress difference, while the HMMSF model with suitable choices of the parameters for dilution modulus and Constraint Release results in a good fit of shear viscosity and N_1 data. In contrast, the DEIA model describes an upper limit of the first normal stress difference data in the high shear-rate regime, which are largely overpredicted by the HMMSF model. We explain this by the effect of arm withdrawal at high deformation rates as reported by Ianniruberto and Marrucci (2013) for entangled melts of branched PS, which behave like linear PS in the steady state of fast flows. The HMMSF model does not take into account the effect of arm retraction. We therefore propose a combination of the HMMSF and the DEIA model by assuming that polymer chain segments with relaxation times τ_i below a threshold value of $\tau_c = 2s$ are so short that they are only oriented, but not stretched. This HMMSF-IA model leads to a transition between the low shear-rate HMMSF and the high shear rate DEIA prediction and results in an improved description of the experimental shear viscosity and N_1 data in the full range of the shear rates investigated. However, further validation of the HMMSF-IA model will be required. We also note that deviations exist between all three models and the $N_1 - N_2$ data obtained by the slit-die circular slot technique in the high shear-rate range. These deviations are associated with the experimental difficulty in assessing small N_2 values with the hole-pressure method.

Funding Open Access funding enabled and organized by Projekt DEAL. The authors acknowledge the financial support by the by Portuguese Foundation for Science and Technology (projects UIDB/05256/2020 and UIDP/05256/2020, and contract CEECINST/00156/2018). EN acknowledges the financial support from the Ministry of Science and Technology of China, MOST Grant # QN2021030003L.

References

Baird DG (1975) A possible method for determining normal stress differences from hole-pressure error data. Trans Soc Rheol 19:147–151. https://doi.org/10.1122/1.549392

Baird DG (2008) First normal stress difference measurements for polymer melts at high shear rates in a slit-die using hole and exit pressure data. J Non-Newton Fluid 148:13–23. https://doi.org/10.1016/j.jnnfm.2007.04.007

Broadbent JM, Kaye A, Lodge AS, Vale DG (1968) Possible systematic error in measurement of normal stress differences in polymer solutions in steady shear flow. Nature 217:55–56. https://doi.org/10.1038/217055a0

Costanzo S, Iannirubertо G, Marrucci G, Vlassopoulos D (2018) Measuring and assessing first and second normal stress differences in polymeric fluids with a modular cone-partitioned plate. Rheol Acta 57:363–376. https://doi.org/10.1007/s00397-018-1080-1

Cyriac F, Covas JA, Hilliou L, Vittorias I (2013) Predicting extrusion instabilities of commercial polyethylene from non-linear rheology measurements. Rheol Acta 53:817–829. https://doi.org/10.1007/s00397-014-0798-7

Dealy JM (2005) Elements of rheology. In: Hatzikiriakos SG, Migler KB (eds) Polymer processing instabilities: control and understanding. Marcel Dekker, New York, pp 30–59

Doi M, Edwards SF (1978) Dynamics of concentrated polymer systems. Part 3. - the constitutive equation. J Chem Soc Faraday Trans 74:1818–1832

Higashitani K, Pritchard WG (1972) Kinematic calculation of intrinsic errors in pressure measurements made with holes. Trans Soc Rheol 16:687–696. https://doi.org/10.1122/1.549270

Iannirubertо G, Marrucci G (2013) Entangled melts of branched PS behave like linear PS in the steady state of fast elongational flows. Macromolecules 46:267–275

Infurna G, Teixeira PF, Dintcheva NT, Hilliou L, La Mantia FP, Covas JA (2020) Taking advantage of the functional synergism between carbon nanotubes and graphene nanoplatelets to obtain polypropylene-based nanocomposites with enhanced oxidative resistance. Europ Polym J 133:109796. https://doi.org/10.1016/j.eurpolymj.2020.109796

Kulicke WM, Jeberien HE, Kiss H, Porter RS (1979) Visual observation of flow irregularities in polymer solutions at theta-conditions. Rheol Acta 18:711–716. https://doi.org/10.1007/BF01533345

Laun HM (1986) Prediction of elastic strains of polymer melts in shear and elongation. J Rheol 30:459–501. https://doi.org/10.1122/1.549855

Meissner J, Garbella RW, Hostettler J (1989) Measuring normal stress differences in polymer melt shear flow. J Rheol 33:843–864. https://doi.org/10.1122/1.550067

Narimissa E, Wagner MH (2016) A hierarchical multi-mode MSF model for long-chain branched polymer melts part III: shear flow. Rheol Acta 55:633–639. https://doi.org/10.1007/s00397-016-0939-2

Narimissa E, Wagner MH (2016) A hierarchical multimode molecular stress function model for linear polymer melts in extensional flows. J Rheol 60:625–636. https://doi.org/10.1122/1.4953442

Narimissa E, Wagner MH (2016) From linear viscoelasticity to elongational flow of polydisperse linear and branched polymer melts: the hierarchical multi-mode molecular stress function model. Polymer 104:204–214. https://doi.org/10.1016/j.polymer.2016.06.005

Narimissa E, Wagner MH (2018) Review of the hierarchical multi-mode molecular stress function model for broadly distributed linear and LCB polymer melts. Poly Eng & Sci 59:573–583. https://doi.org/10.1002/pen.24972

Narimissa E, Wagner MH (2019) Review on tube model based constitutive equations for polydisperse linear and long-chain branched polymer melts. J Rheol 63:361–375. https://doi.org/10.1122/1.5064642

Narimissa E, Rolón-Garrido VH, Wagner MH (2015) A hierarchical multi-mode MSF model for long-chain branched polymer melts part I: elongational flow. Rheol Acta 54:779–879. https://doi.org/10.1007/s00397-015-0879-2

Narimissa E, Rolón-Garrido VH, Wagner MH (2016) A hierarchical multi-mode MSF model for long-chain branched polymer melts part II: multiaxial extensional flows. Rheol Acta 55:327–333. https://doi.org/10.1007/s00397-016-0922-y

Narimissa E, Schweizer T, Wagner MH (2020) A constitutive analysis of nonlinear shear flow. Rheol Acta 59:487–506

Olley P, Gough T, Spares R, Coates PD (2022) 3D simulation of the hierarchical multi-mode molecular stress function constitutive model in an abrupt contraction flow. J Non-Newtonian Fluid Mech 304:104806. https://doi.org/10.1016/j.jnnfm.2022.104806

Poh L, Narimissa E, Wagner MH, Winter HH (2022) Interactive shear and extensional rheology - 25 years of IRIS Software. Rheol Acta 61:259–269. https://doi.org/10.1007/s00397-022-01331-6

Schweizer T (2002) Measurement of the first and second normal stress differences in a polystyrene melt with a cone and partitioned plate tool. Rheol Acta 41:337–344. https://doi.org/10.1007/s00397-002-0232-4

Schweizer T (2003) Comparing cone-partitioned plate and cone-standard plate shear rheometry of a polystyrene melt. J Rheol 47:1070–1085. https://doi.org/10.1122/1.1584428

Snijkers F, Vlassopoulos D (2011) Cone-partitioned-plate geometry for the ARES rheometer with temperature control. J Rheol 55:1167–1186. https://doi.org/10.1122/1.3625559

Tanner RI, Keentok M (1989) Shear fracture in cone-plate rheometry. J Rheol 27:47–57. https://doi.org/10.1122/1.549698

Teixeira PF, Hilliou L, Covas JA, Maia JM (2013) Assessing the practical utility of the hole-pressure method for the in-line rheological characterization of polymer melts. Rheol Acta 52:661–672. https://doi.org/10.1007/s00397-013-0695-5

Teixeira PF, Fernandes SN, Canejo J, Godinho MH, Covas JA, Leal C, Hilliou L (2015) Rheo-optical characterization of liquid crystalline acetoxypropycellulose melt undergoing large shear flow and relaxation after flow cessation. Polymer 71:102–112. https://doi.org/10.1016/j.polymer.2015.06.056

Teixeira PF, Maia JM, Covas JA, Hilliou L (2015) A small-scale experimental extrusion set-up for exploring relationships between process-induced structures and characteristics of multiphase polymer systems. Macromol Mater Eng 12:1278–1289. https://doi.org/10.1002/mame.201500196

Teixeira PF, Ferrás LL, Hilliou L, Covas JA (2018) A new double-slit rheometrical die for in-process characterization and extrusion of thermo-mechanically sensitive polymer systems. Polym Test 66:137–145. https://doi.org/10.1016/j.polymertesting.2018.01.013

Teixeira PF, Covas JA, Hilliou L (2020) In-process assessment of clay dispersion in PLA during melt compounding: effects of screw speed and filler content. Polym Degrad Stabil 177:109190. https://doi.org/10.1016/j.polymdegradstab.2020.109190

Teixeira PF, Covas JA, Hilliou L (2021) In-line rheo-optical investigation of the dispersion of organoclay in a polymer matrix during

twin-screw compounding. Polymers 13:2128. https://doi.org/10.3390/polym13132128

Wagner MH, Narimissa E, Poh L, Huang Q (2022) Modelling elongational viscosity overshoot and brittle fracture of low-density polyethylene melts. Rheol Acta 61:281–298. https://doi.org/10.1007/s00397-022-01328-1

Wagner MH (2022) Private communication.

Winter HH, Mours M (2006) The cyber infrastructure initiative for rheology. Rheol Acta 45:331–338. https://doi.org/10.1007/s00397-005-0041-7

You W, Yu W (2021) Characteristic rheological behaviors in startup shear of entangled polymer melts. Nihon Reoroji Gakkaishi 49:1–5. https://doi.org/10.1678/rheology.49.1